Indonesian Journal of Electrical Engineering and Informatics (IJEEI)
Vol. 13, No. 1, March 2025, pp. 261~276
ISSN: 2089-3272, DOI: 10.52549/ijeei.v13i1.5211

Dual Band Circular Polarized Design of Rectangular Microstrip Antenna For GPS L-band and Galileo E-band Applications

Amit A. Deshmukh[1], Tejal P. Page[2], Venkata A. P. Chavali[3]
[1]Professor & Head, EXTC, DJSCE, Mumbai University, Mumbai, Maharashtra, India
[2]Research Scholar, EXTC, DJSCE, Mumbai University, Mumbai, Maharashtra, India
[3]Assistant Professor, EXTC, DJSCE, Mumbai University, Mumbai, Maharashtra, India

Article Info

Article historys:

Received Jan 3, 2025
Revised Mar 12, 2025
Accepted Mar 25, 2025

Keywords:

Circular polarization
Rectangular microstrip antenna
Dual band microstrip antenna
Multiple rectangular slots

ABSTRACT

Design of rectangular microstrip antenna employing three rectangular slots of unequal lengths on one of the patch edges, is presented to achieve dual band and dual sense circular polarized characteristics. Circular polarized response in the two bands is attributed to the optimum inter-spacing in between the rectangular patch's TM_{10}, TM_{11} and TM_{12} resonant modes. For axial ratio less than 3 dB, an optimum design offers axial ratio bandwidth of 26 MHz (2.05%) and 73 MHz (4.59%) in the dual bands, bearing frequency ratio of 1.25. This circular polarized bandwidth lies inside the VSWR $\leq$ 2 bandwidth of 665 MHz (49.83%). Antenna offers radiation pattern maximum in the broadside direction across axial ratio and VSWR bandwidth, with a gain of more than 6 dBic. For the obtained antenna characteristics, the three rectangular slot cut design is suitable in variety of applications like, GPS L1 & L2 bands, and Galileo E1 & E6 bands. The experimental verification has been carried out for the proposed configuration that shows close agreement against the simulated results.

Corresponding Author:

Amit A. Deshmukh,
Department of Electronics and Telecommunication Engineering,
SVKM's D J Sanghvi College of Engineering,
Vile – Parle, Mumbai, Maharashtra, India.
Email: amitdeshmukh76@gmail.com

1. INTRODUCTION

Owing to the various advantages like, small volume, low-cost design, microstrip antenna (MSA) finds more applications in wireless communication [1, 2]. The transmitted signal travels through the multiple paths in wireless propagation that leads to a reduction in signal strength at the receiver; mainly attributed to the mismatch in between polarization of incoming wave against the receiver antenna. To overcome this loss, antenna offering high value of cross-polar level in the polar radiation pattern plot is used. This pattern requirement needs the design of elliptically polarized or circular polarized (CP) antennas. Amongst the two, CP antennas show minimum signal loss as it receives the signal from all orientation of the incoming radio waves [2]. To realize the CP radiation, three conditions namely, equal amplitude, time and space orthogonal signals are needed [2]. While using MSAs, narrow or wideband CP characteristics are realized by placing slot and stub on the edges of the patch [3 – 8], shorting posts loaded MSAs [9 – 11], radiating patch employing modified shape [12, 13], use of gap-coupled parasitic patches with the fed patch [14, 15], using printed filter elements feeding the main patch [16] and use of delay line fed design offering dual sense CP response [17]. The U-slot, rectangular slot and their variations are reported in the literature to yield wideband linear polarized response [4]. These slot-cut variations are explored on thicker air suspended microwave substrate, to achieve the CP response that offers bandwidth (BW) of 4 – 5% for axial ratio (AR) lower than 3 dB [18 – 21]. The modified Ψ-shape MSA design is reported [22] that offers wider AR BW. However, this configuration is complex in design and does not offer CP characteristics in the broadside direction. This gives an alignment

problem of the antenna against the incoming wave. A modified ground plane design by employing fractal variations of U-slot is reported [23]. Although it is a low-profile design, but it offers narrow AR BW.

In case of signal interference/jamming, the MSA operating band is required to be switched. In this scenario, a single band CP design is not useful. Here, dual band CP MSAs are selected. The dual band CP characteristics is obtained by tuning the spacing in between the patch's fundamental and higher order resonant mode frequencies. This is realized either by loading the patch edges with an open circuit stubs [24, 25], or by using the multi-resonator gap-coupled planar design [26], or by employing modified patch shapes [27, 28], or by using the combination of shorting post and slots [29, 30], or by placing additional patches in the layer above the fed patch layer (stacked designs) [31, 32], or by employing modified shape slots in the patch [33], or by employing the meta surface materials [34]. The use of stubs in the patch or additional patches in the stacked or planar design increases the patch area, whereas in the modified patch shape designs, details about the antenna functioning in terms of resonant modes of the patch is not described. Combination of short and slot together or the design with meta surface, increases the design complexities. The dual band dual sense design reported in [33] is a single patch variation, but it does not offer CP characteristics in the broadside direction. Amongst various methods to realize single and dual band CP characteristics, resonant slot cut design is the efficient one, as it offers moderately high value of the reflection coefficient (S_{11}) & AR BW, with a broadside gain $\geq$ 6 dBic, using a simple coaxially fed single patch design.

Based on the above mentioned research gaps observed in the reported dual band CP MSAs, a design of rectangular MSA (RMSA) using three unequal lengths rectangular slots is proposed in this work, to obtain a dual band and dual sense CP response, in the broadside direction. Initially, a detailed explanation about selecting the proposed geometry to achieve the desired characteristics is presented. Further, a parametric study is presented that explains the three rectangular slots effect on RMSA resonant modes. Multiple slots in the patch alters the resonance frequencies and impedances across all the resonant modes and further yields optimum separation between TM_{10}, TM_{11} and TM_{12} modes, which yields dual band CP characteristics. On substrate of thickness $0.07\lambda_g$, proposed design yield simulated AR BW of 26 MHz (2.05%) and 73 MHz (4.59%) in the dual bands, bearing a frequency ratio of 1.25, and which lies inside 665 MHz (49.83%) of the S_{11} BW. Over the AR and S_{11} BW, MSA exhibits broadside radiation pattern, showing broadside gain greater than 6 dBic. The antenna characteristics have been experimentally verified, which shows a close agreement against the simulated results. For re-designing the antenna, simpler parametric formulations based on the optimum design of the dual band dual sense RMSA, are presented. Using the same, a procedure is put forward to design similar antenna to cover either GPS L1 & L2 bands, or Galileo E1 & E6 bands. This yields similar dual band dual sense CP results thus satisfying the requirement of the practical applications. Thus, the proposed study presents a coaxially fed single layer single patch configuration for the CP response in dual bands that offer CP characteristics in the broadside directions against the previously reported resonant slots cut CP MSAs. A tabular comparison for different antenna parameters, presenting the novelty in the proposed MSA against the reported one using different CP techniques is discussed ahead. Dual band slot cut RMSAs proposed here are initially studied using CST simulations [35]. An experimental verification is carried out inside the Antenna laboratory, using instruments namely, FSC 6, SMB 100A and ZVH – 8. The square ground plane having 40 cm side length and N-type feed of 0.16 cm inner wire radius is selected in the present study.

2. Dual band CP Design of Rectangular slots loaded RMSA

Owing to the single patch thicker substrate design, the resonant slot cut MSAs offers optimum solution to realize CP response with moderately high value of AR BW and gain. In slot cut broadband MSAs, the slot length and its position ensure uni-directional modal surface currents on the patch that realizes broadside radiation pattern with a linear polarization over the S_{11} BW. Against these, in resonant slot cut CP MSAs, slot parameters ensure surface current variation along both the dimensions on slot cut patch that assist in the generation of CP wave [18 – 20]. Initially in the literature, slot cut MSAs for single band CP response were reported. By embedding additional slots in the slot cut MSA, either a wideband CP response [22] or a CP response in the two bands [33], has been achieved. In multiple slots cut CP MSAs, since higher order resonant modes are present to yield circular polarized characteristics, the same is obtained in the direction away from the broadside [22, 33]. This poses an antenna alignment problem against the incoming radio waves. When multiple slots are cut in the patch along both of its dimensions, they alter the higher order modal currents along the patch length as well as width [33, 36]. Because of these modified higher order modal currents along the two patch dimensions, CP response is observed in the direction away from the broadside. However, if slots are present only along one dimension in the patch, they will primarily alter the current components along one direction and will have minimum effect on the currents in the other direction. Further, by exploring two-dimensional vector current variation on the slot cut patch at some of its modified higher order resonant modes (e.g., TM_{12}), the slots present along one axis inside the MSA, can also give the CP response in the broadside direction.

Based on this insight, multiple slots cut design of RMSA is explored here to realize dual band circular polarized response in the broadside direction, as given in Fig. 1(a, b). In the proposed design, three unequal lengths rectangular slots are cut on one of the patch edges and an offset coaxial feed position is considered. Unlike the reported MSAs, multiple slots are placed only along length of the RMSA. At higher order orthogonal modes, integer multiples of half wavelength variation are present along RMSA width, with bi-directional current variations at some of the modes (e.g. TM_{12}). Hence, the selection of closely spaced three rectangular slots will assist in the tuning of more than one higher order resonant mode with reference to the fundamental patch mode. Tuning of more than one resonant mode is essential to yield dual band characteristics [33]. As depicted in Fig. 1(d – g), in some of the higher order modes, slots along RMSA length will increase modal surface current lengths along the RMSA width. In resonant modes showing current variation along both the dimensions in patch, slot lengths will tune their frequency with reference to fundamental mode and will yield current variations along two RMSA dimensions, so as to assist the generation of circular polarized wave. It should be noted here that driven patch modes are considered, which are the function of feed location. The chartacteristics mode theory is not considered in this study as it is independent of the feed location. The two dimensional current variation on RMSA will be strengthened in magnitude with the selection of an offset feed position. Thus, keeping all these factors in consideration, proposed slot cut design is selected. For better illustrating the design, simulated 3D-isometric view of the slots cut RMSA obtained using CST software is provided in Fig. 1(c). For an air gap of h_a = 1.8 cm, using air suspended low cost FR4 substrate (ε_r = 4.3, h = 0.16 cm) and by employing CST simulation, RMSA length 'L' is optimized for f_{TM10} = 1100 MHz. Using the simulation, length is found to be 9.8 cm and width 'W' is selected as 12.2 cm. This gives W/L = 1.245, which realizes moderate value of the gain, while using a single patch design [3].

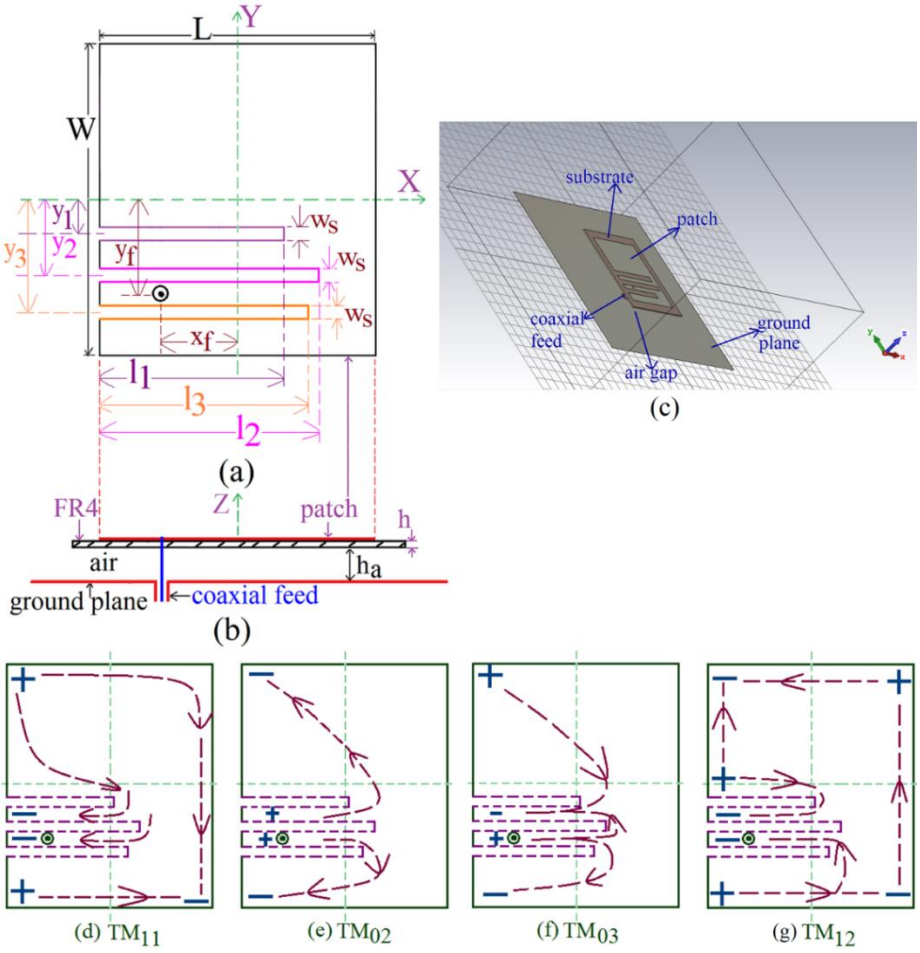

Figure 1. (a, b) Multiple rectangular slots loaded RMSA and its (c) simulated 3D isometric view, field & current distributions at the modified (d) TM_{11}, (e) TM_{02}, (f) TM_{03} and (g) TM_{12} resonant modes.

To analyse the effects of slots on the excitation of higher order orthogonal RMSA resonant modes, parametric variations for three rectangular slot lengths is carried out. Resonance curve plots for this variation, for y_1 = 0.8, y_2 = 2.5, y_3 = 4.2, w_s = 0.9, x_f = 2.6, y_f = 3.3 cm, are shown in Fig. 2(a – c).

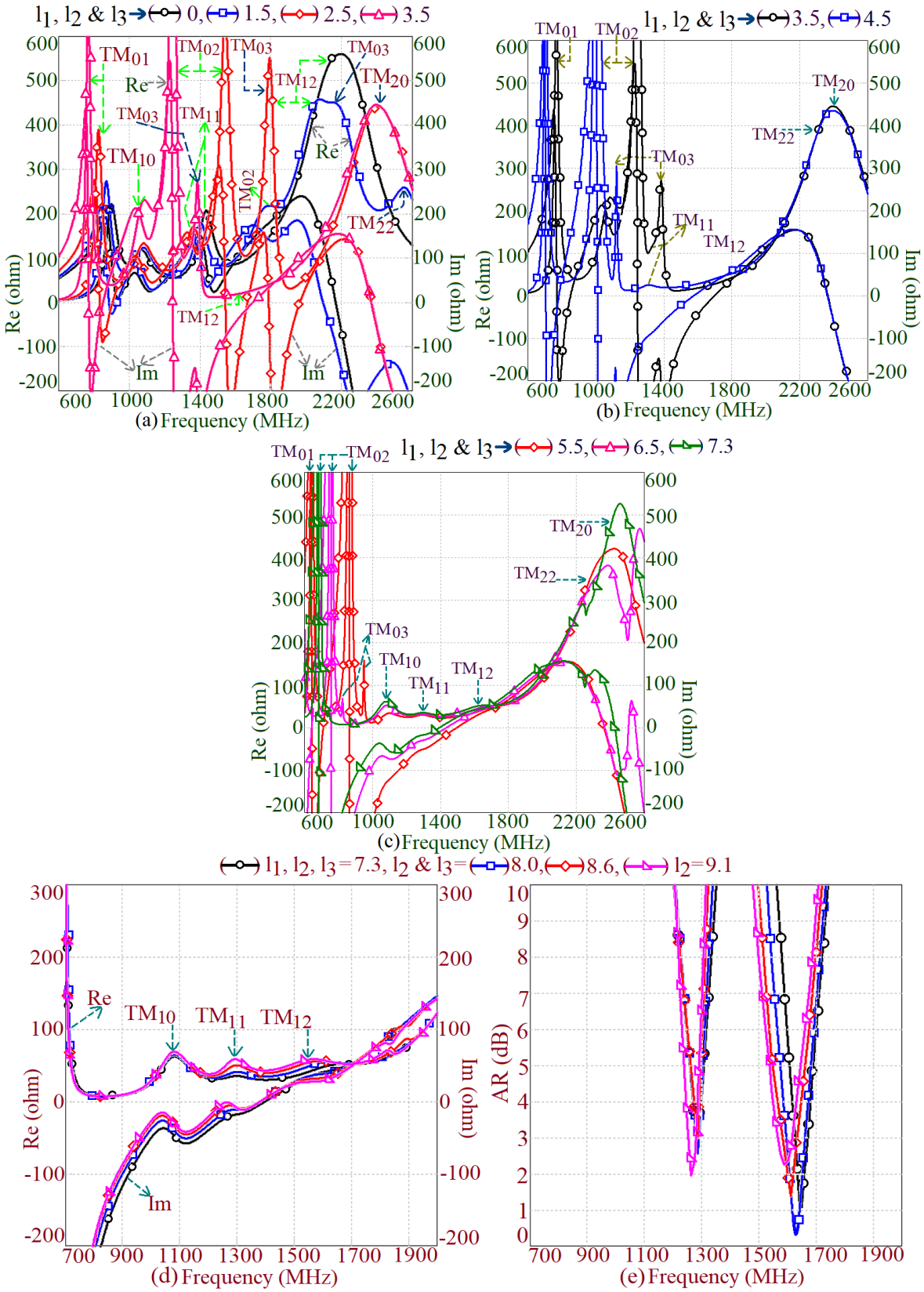

Figure 2. (a – d) Resonance curve plots and (e) axial ratio variations against the slot lengths increments for multiple rectangular slots loaded RMSA.

Initially slot lengths 'l_1', 'l_2' and 'l_3', are increased together in steps up till 7.3 cm. Later, only lengths 'l_2' and 'l_3' and then length 'l_2' are increased. As observed in the parametric study, unequal lengths for the

three slots are considered as it helps in optimizing the frequency separation and impedance at various resonant modes to give AR values lower than 3 dB for the CP response. The frequencies of various resonant modes are governed by the patch length and width. The slot position alters the current distributions at each resonant mode that changes their current path length and thus the effective patch dimensions. This effect is more for those modes, which have their current components orthogonal to the increasing slot length. The resonance plots are shown for wide frequency range as that depicts the variations in frequencies of fundamental and various higher order modes. The modal currents at TM_{01}, TM_{02}, TM_{12}, TM_{03} and TM_{22} mode frequencies are orthogonal to three slot lengths, hence their frequencies reduce with an increase in 'l_1', 'l_2' & 'l_3'. The appearance of each resonant mode in the resonance curve is confirmed by observing the vector current distributions in each slot length variation as well as their variation in frequency value against the increment in length of the slot. Initially, with the increase in slot lengths, TM_{01} mode frequency decreases. A larger decrease in the frequencies of TM_{02} and TM_{03} modes is noted as the modal currents varying along width of RMSA shows two and three half wavelength variations, respectively. For slot lengths more than 6.5 cm, frequencies of these two modes reduces below TM_{10} mode frequency. The frequency of TM_{20} mode appears to be increasing with the slot lengths. At TM_{20} mode, vector currents along the RMSA length show two half wavelength variation. Because of this, against the slot lengths increment, effective length as seen by the surface currents over the patch length 'L' reduces that increases their frequency. Similar effect is also observed for TM_{22} mode frequency, due to their vector current components along the RMSA length. Further, with increments in slot lengths 'l_2' & 'l_3' and later only 'l_2', frequencies of various modes marginally change, as depicted in Fig. 2(d). But these lengths variation yields minimum value of AR, in the two operating bands to yield the dual band CP characteristics as given in Fig. 2(e). As can be noted from the resonance plot given in Fig. 2(d), across modified TM_{10}, TM_{11} and TM_{12} modes, impedance level remains below 100 Ω that yields impedance matching for $S_{11} \leq$ -10 dB, to yield maximum possible BW and inside which the circular polarized AR BW is obtained.

Thus, unequal slot lengths, yields impedance matching as well as minimum values of the AR, to yield optimum dual band CP response as given in Fig. 3(a). The S_{11} BW noted in the simulation and measurement is, 665 MHz (49.83%) and 685 MHz (51.87%), respectively. The CP BW showing AR value lower than 3 dB observed in the simulation in dual bands are, 26 MHz (2.05%) and 73 MHz (4.59%). Respective AR BW observed in the measurement are, 28 MHz (2.24%) and 69 MHz (4.39%). As against the reported multiple slots cut RMSA, this CP BW is observed in the direction perpendicular to the antenna plane, i.e., broadside. Dual band CP RMSA shows broadside gain of greater than 6 dBic over the AR and S_{11} BW, with a peak value of 9 dBic. The 3D radiation pattern plot in the simulation and 2D polar pattern plots observed in the simulation and measurement, at the center frequency of two CP bands provided in Fig. 3(b – g), exhibits pattern maxima in the broadside direction. Because of the CP nature of radiation from the antenna, level of the cross-polar component is within 3 dB difference with reference to the co-polar levels, as noted in the broadside direction.

Simulated time varying surface current distribution and right and left-hand field polarization plots at the center frequencies of dual bands is provided in Figs. 4 & 5(a – d). In the first band, right hand field components are higher in magnitude with vector surface currents rotating in an anti-clock wise direction. This confirms presence of right-hand CP (RHCP) wave. Polarization plots in the second band, shows higher magnitude left hand CP (LHCP) field components with patch surface currents rotating in the clockwise direction, to confirm the LHCP radiation. The simulated plot for the ratio of orthogonal field components (E_x/E_y) against the phase difference between respective components ($\Phi_x - \Phi_y$) is shown in Fig. 5(e – g). Nearer to the two frequency bands, value of E_x/E_y is unity and phase difference between the two components '$\Phi_x - \Phi_y$' is around -270^0 and -90^0. These two frequency bands are nearer to the frequencies where CP response for AR $\leq$ 3 dB is noted. In the first CP band '$\Phi_y - \Phi_x$' equals 270^0. With reference to the vector field distribution provided in Fig. 5(f), effective field vector will rotate in an anti-clockwise direction against the time, thereby realizing RHCP wave. Similarly, in the second band '$\Phi_y - \Phi_x$' equals 90^0 that will give the field distribution as shown in Fig. 5(g). This with time variation will give LHCP wave. Thus, in addition to the radiation pattern and time varying current vector plots, field and phase plots further confirms the presence of CP response in the dual bands. Sense of rotation in dual bands is confirmed in the measurements, by employing nearly square MSA (SMSA) as the transmitting antenna, operating in either LHCP or RHCP mode. In the broadside direction of measurement, when sense of rotation of slot cut CP RMSA matches with the transmitter SMSA, then the received power is maximum. When there exists a mismatch, i.e., transmitter excited in the opposite sense of rotation than the dual band CP antenna, then the received power reduces below 8 – 10 dB. This confirms the RHCP or LHCP response experimentally.

The fabricated prototype of the dual band RMSA, S_{11} BW, radiation pattern, axial ratio and broadside gain measurement setup are provided in Fig. 6. The antenna response is experimentally verified inside the Antenna laboratory. In all the far field measurements, a distance of more than '$2D^2/\lambda$' is maintained. Here 'D' is selected as the diagonal ground plane length, which is the largest dimension present. Here 'λ' is the wavelength nearer to the highest frequency of the S_{11} BW.

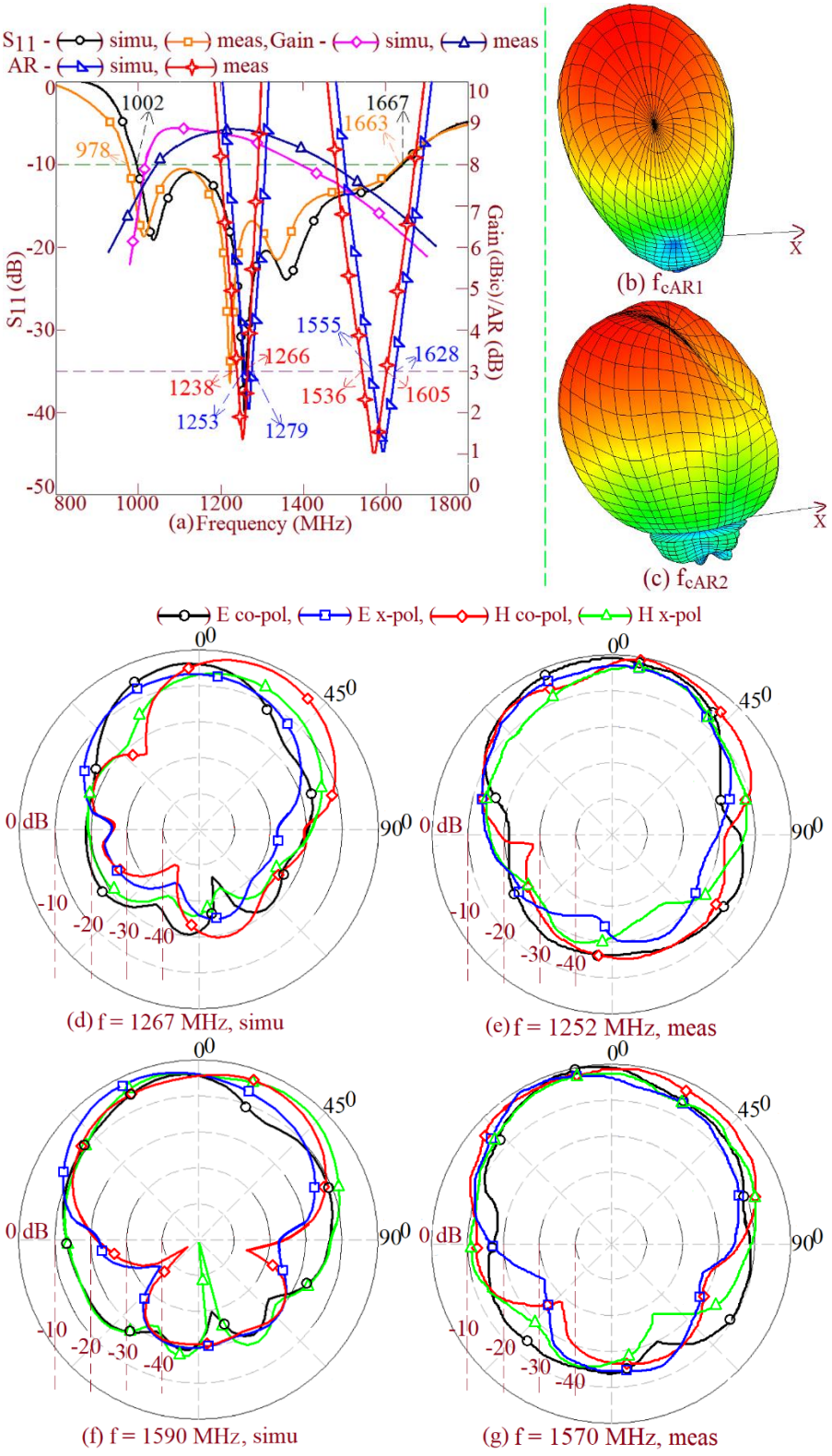

Figure 3. (a) S_{11}, AR BW and gain plots, (b, c) 3-D radiation pattern plots in two CP bands, and (d - g) 2D polar radiation pattern plots at the center frequency of the two CP bands for multiple slots loaded RMSA.

As can be seen in Fig. 6(d), with reference to measurement setup shown in the center, no surrounding metal objects are present around the line joining the transmitter and receiver. The distance of surrounding objects with respect to the Antenna measuring desk is more than 8λ, where 'λ' is measured with reference to the lowest frequency of the S_{11} BW. This measurement setup ensures minimum reflection environment.

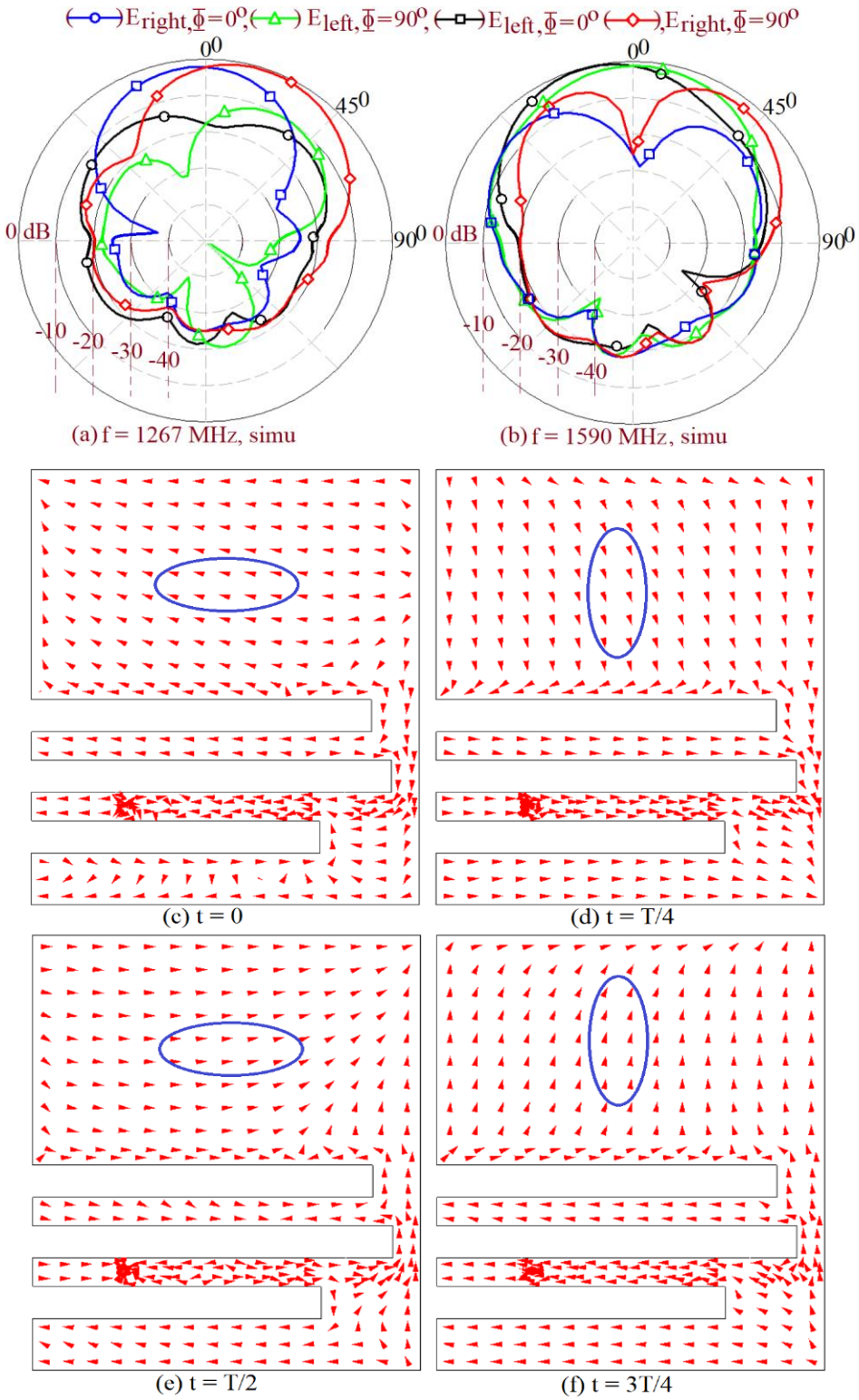

Figure 4. (a, b) Polarization plots nearer to the center frequencies of two CP BW and (c – f) varying current distribution over the time nearer to the center frequency of first CP band for dual band multiple slots loaded RMSA.

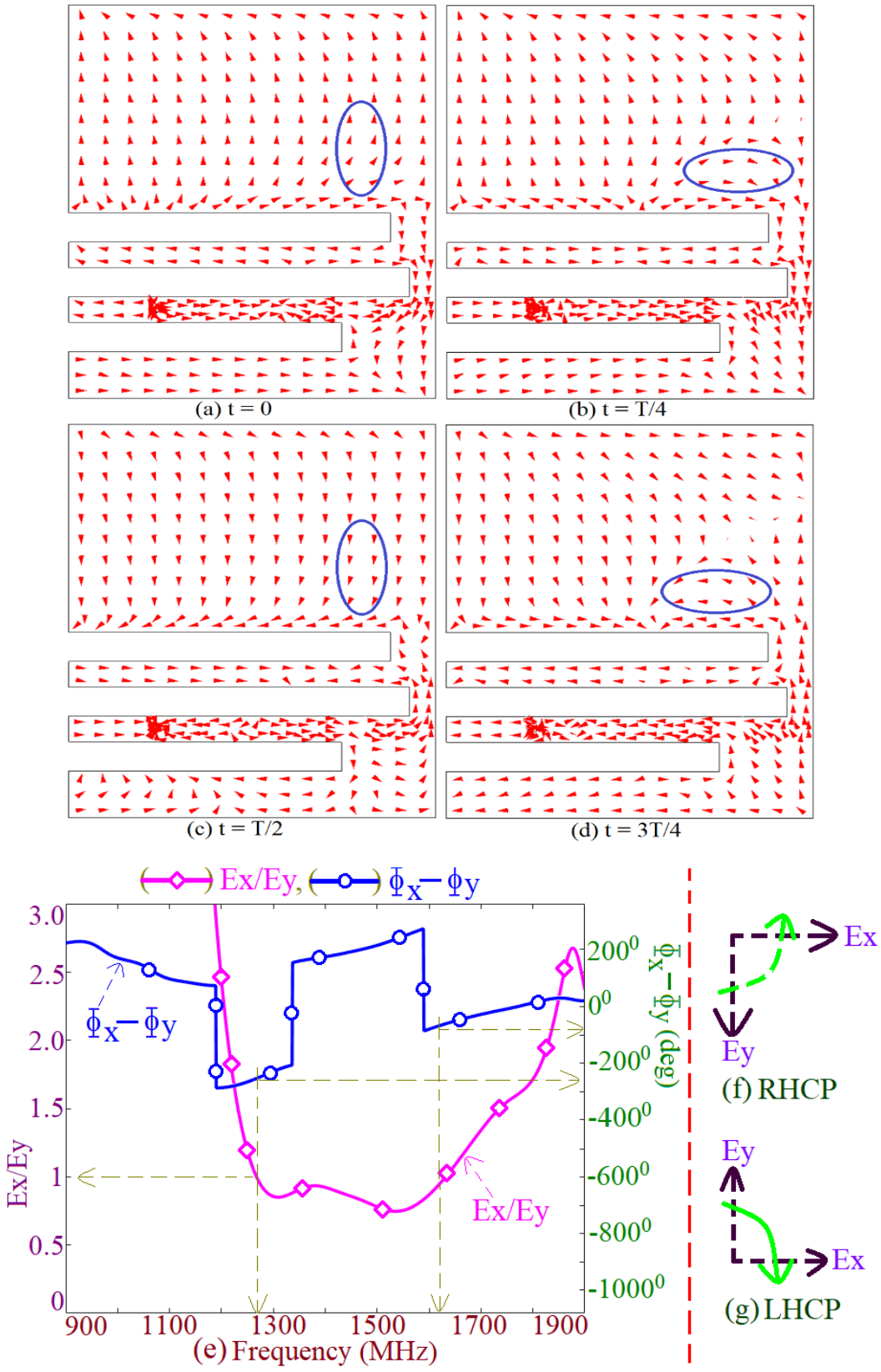

Figure 5. (a – d) Varying surface current distributions over the time at the center frequency of the second CP band and (e) amplitude and phase difference plots between two orthogonal fields against the frequencies and time varying electric field vectors for (f) RHCP and (g) LHCP response for dual band multiple slots loaded RMSA.

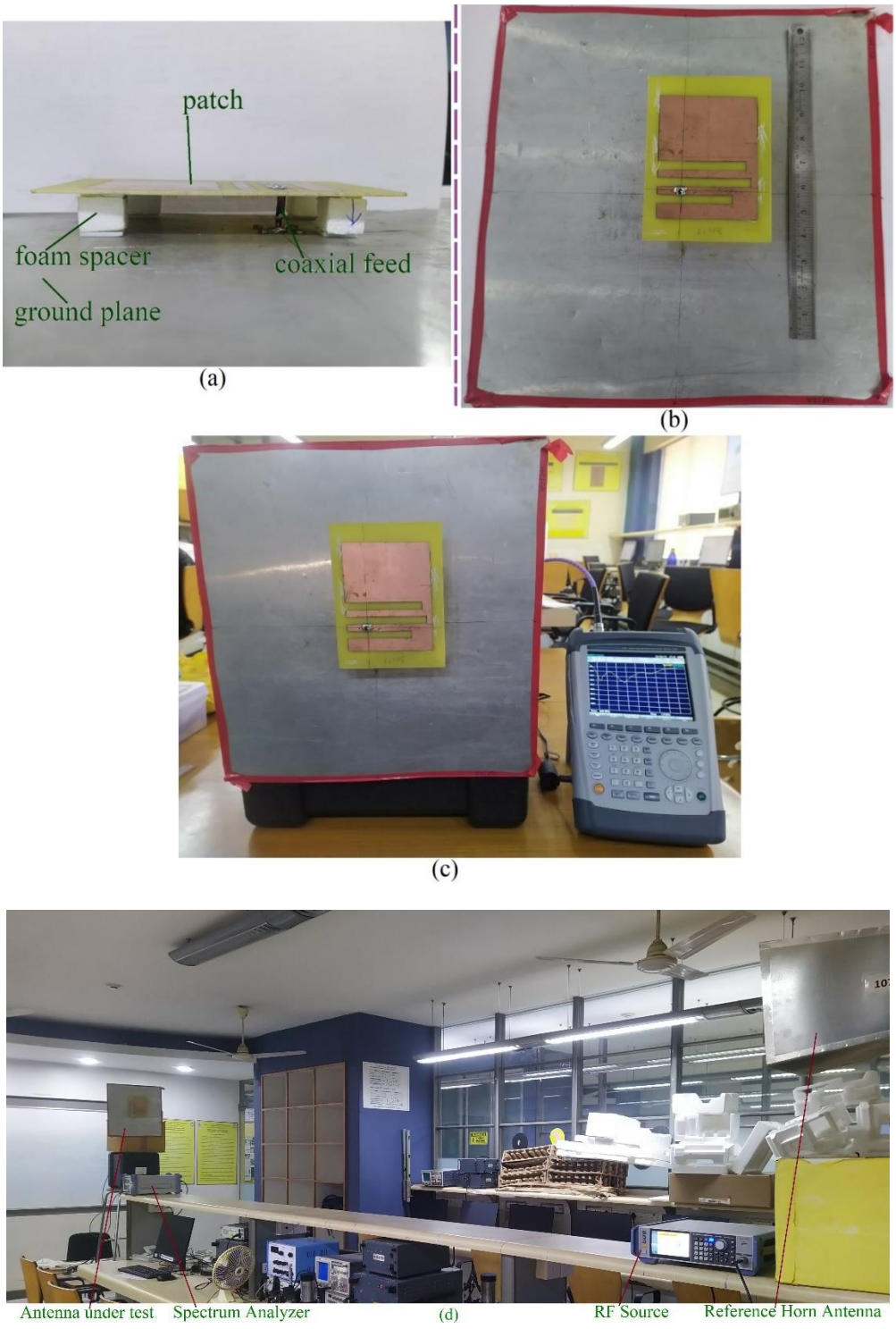

Figure 6. (a, b) Fabricated prototype, (c) impedance measurement and (d) pattern, axial ratio and gain measurement setup for the dual band multiple slots loaded RMSA.

Broadside antenna gain is measured using three-antenna method, where along with the proposed dual band antenna, two wideband high gain Horn antennas have been used. Three-antenna gain method provides a better accuracy in the gain measurement in the lab environment and against any variation in the gain of two reference antennas. In AR BW measurement, initially for each band, identification of the two planes of measurement is carried out by rotating the antenna in 'Φ' direction. The plane is fixed, where the maximum received power amongst all the angles is received. Then the measurement of the received power is carried out over the axial ratio and S_{11} BW in this plane and in the plane orthogonal to this identified plane. Across the frequency spectrum where circular polarization is present, the difference between the received power (in dB)

in the two orthogonal planes is very small, thus indicating the presence of CP response. Beyond these frequency spectrums, the difference between the two power levels is more than 6 – 8 dB.

Proposed dual band CP antenna gives RHCP response in first band and LHCP characteristics in the second band. This sense of rotation in each band is altered by changing the slot positions, as given in Fig. 7(a, b). MSA shown in Fig. 7(b), will realize LHCP in the first band and RHCP in second band. Initially in the present study, square ground plane dimensions are selected as 40 x 40 cm. A large ground plane size is selected as that simulate the effects of infinite ground plane. Study was also carried out with a smaller ground plane dimensions, such as 40 x 40 (initial), 30 x 30, 24 x 24 and 18 x 18 cm. The S_{11} BW plots for the various ground plane dimensions are shown in Fig. 7(c). The wideband response with CP in the two bands is obtained in all the cases. However, for smaller ground plane dimensions, i.e. $\leq$ 18 x 18 cm, the impedance at various resonant mode increases. This increases the S_{11} value above -10 dB, as well as it increases the AR value in the two bands above 3 dB. To achieve the impedance matching over S_{11} BW and to realize AR $\leq$ 3 dB, minor parametric optimization in the three rectangular slot lengths is needed that alters the input impedance at various resonant modes present, to yield optimum dual band CP characteristics. Thus, dual band circular polarized response can be obtained in all the ground plane dimensions. Further, based on the optimum configuration, methodology to design similar dual band antennas is presented.

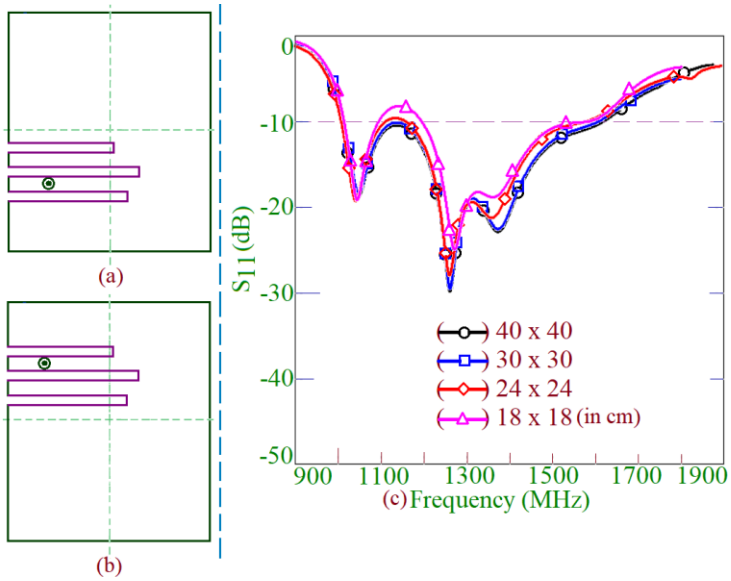

Figure 7. Three rectangular slot cut design for (a) RHCP and (b) LHCP response in the first band, (c) S_{11} plots for varying ground plane dimensions

3. Design Methodology for Slots cut Dual band CP RMSA

As noted from the above optimum results, CP response in dual band three rectangular slots cut RMSA is present around the modified TM_{11} and TM_{12} mode frequencies. To calculate the RMSA dimensions, these modified resonant mode frequencies cannot be used since they include rectangular slots effects on the modes. As noted from the above parametric study, against increment in the slot lengths, TM_{10} mode frequency remains constant. Thus, based on the optimum design above, frequency ratio between center frequency of first CP band (f_{cp1}) and TM_{10} mode frequency in slot cut patch as given in equation (1) is used to calculate the RMSA dimension. A suspended substrate of total thickness $0.072\lambda_g$ is selected. At the given TM_{10} mode frequency, its value is obtained by using equation (2). Here 'ε_{re}' represents effective dielectric constant calculated for the suspended substrate. Initially, the 'ε_{re}' value is unknown. Since the thicker substrate is used, an approximation of $\varepsilon_{re} = 1.06$, is considered. As 'h_t' equals '$h + h_a$', from the value of 'h_t' as obtained using (2), for FR4 substrate, value of 'h_a' that is practically realizable, is considered. For this value, using the capacitance formula [1], 'ε_{re}' is re-calculated. As thicker substrate is used, marginal variations in the re-calculated 'ε_{re}' value from the initial assumption is noted. Hence, an initially assumed value of 'ε_{re}' is used in further calculations. At the given TM_{10} mode frequency, RMSA length and width are calculated using equations (3) & (4).

$$f_{10} = {}^{f_{cp1}}\!/_{1.185} \quad (1)$$

$$h_t = 0.072\left(\frac{30}{f_{10}\sqrt{\varepsilon_{re}}}\right) \quad (2)$$

$$L = \left(\frac{30}{2f_{10}\sqrt{\varepsilon_{re}}}\right) - 1.9h_t \quad (3)$$

$$W = 1.245L \quad (4)$$

The three slot lengths in the dual band CP RMSA affects the TM_{11}, TM_{12} mode frequencies around which the CP response is present. The effects of the lengths on the frequencies have been established in the parametric study above, by observing the resonance curve and surface current plots. However, due to the close proximity of the three slots, formulating their effects individually on the resonant length at TM_{11} and TM_{12} modes was difficult to achieve. Hence, the parametric relation for the slot parameters is used to calculate their dimensions at other frequencies. Thus, based on the three rectangular slots parameters in the optimum design above, slot lengths, 'l_1', 'l_2' and 'l_3' are selected as, 0.8775L, 0.9286L and 0.7449L, respectively. These slots are placed at the position of 'y_1', 'y_2' and 'y_3' of 0.066W, 0.205W and 0.344W, respectively, from the RMSA center axis. Width of the slot is selected as 0.074W. From the patch origin, coaxial feed point location is selected as, x_f = 0.2653L, y_f = 0.27W.

In the optimum design above, frequency ratio with reference to the center frequencies in the two circular polarized bands (f_{cp2}/f_{cp1}) is 1.257, where it offers AR BW of 2 and 4.5%, respectively. In wireless applications like, GPS L1 & L2 and Galileo E1 & E6, a CP antenna is needed that reduces the signal loss. Thus, using the proposed design methodology, dual band CP RMSA that is design to cater to GPS L1 & L2 bands and Galileo E1 and E6 bands is presented. The GPS L1 frequency band is centered around 1575 MHz with a BW of 15 MHz, whereas L2 band is centered around 1228 MHz with a BW of 11 MHz. In Galileo bands, E1 band is centered around 1575 MHz with a BW of 32 MHz, whereas E6 band is centered around 1279 MHz with a BW of 40 MHz. In these applications, frequency ratio between the two CP bands is around 1.25, which satisfies the proposed dual band antenna specifications.

For realizing the two designs, center frequency of the first circular polarized band 'f_{cp1}' is selected as 1228 MHz, in GPS application and 1279 MHz in Galileo application. Using equation (1), corresponding TM_{10} mode frequency in each design is obtained. By using equations (2) – (4), total substrate thickness and corresponding value for the air gap thickness 'h_a', and RMSA dimensions i.e. length and width, are calculated. By using the parametric equation for various slot lengths and coaxial feed parameters as mentioned above, their values for each of the design are calculated. Using the above procedure, antenna parameters as calculated for GPS dual band CP design are, h_a = 1.9, L = 10.1, W = 12.6, l_1 = 8.9, y_1 = 0.8, l_2 = 9.4, y_2 = 2.6, l_3 = 7.6, y_3 = 4.35, w = 0.9, x_f = 2.7, y_f = 3.4 cm. Similarly, the antenna parameters for the Galileo dual band CP design are, h_a = 1.9, L = 9.7, W = 12.1, l_1 = 8.55, y_1 = 0.8, l_2 = 9.05, y_2 = 2.5, l_3 = 7.25, y_3 = 4.2, w = 0.9, x_f = 2.6, y_f = 3.3 cm. The results for the S_{11} & AR BW, broadside gain in the two configurations, are provided in Fig. 8(a, b). For the RMSA realizing two Galileo bands, E1 and E6, S_{11} BW observed in simulation and measurement is 669 MHz (49.65%) and 685 MHz (50.98%), respectively. CP AR BW in the two bands observed in the simulation are, 34 MHz (2.66%) and 68 MHz (4.24%), respectively. In measurements, AR BW noted in two bands is 36 MHz (2.83%) and 78 MHz (4.89%). Antenna offers broadside gain greater than 6 dBic over the entire S_{11} and AR BW. Antenna peak broadside gain is close to 9 dBic. Similarly, in dual band RMSA realizing two GPS bands L1 and L2, S_{11} BW noted in simulation and measurement is 624 MHz (48.3%) and 646 MHz (50.27%), respectively. In this design, AR BW observed in the simulation in dual bands is, 33 MHz (2.68%) and 69 MHz (4.46%), respectively. In measurements, AR BW obtained in dual bands is 40 MHz (3.27%) and 75 MHz (4.87%), respectively. This design also offers broadside gain greater than 6 dBic over the entire S_{11} BW, with a peak value of 9 dBic. With reference to the results obtained here, both the designs satisfy the requirement of GPS L1 & L2 and Galileo E1 (1559 MHz to 1591 MHz) & E6 (1260 MHz to 1300 MHz) frequency spectrums. A close matching in two band frequencies against the desired one is achieved.

4. Results Discussion and Comparative Analysis

To highlight upon the novelty in the proposed design, a tabular comparison against the reported CP designs offering single and dual band response is given in Table I. For comparing antenna size amongst different designs, total substrate thickness (h_t) and MSA area (A_p) is provided in Table I, and it is being normalized with reference to wavelength at the center frequency of axial ratio BW in the first CP band. This normalization helps in comparing the antenna size amongst different designs that is independent of frequency of operation.

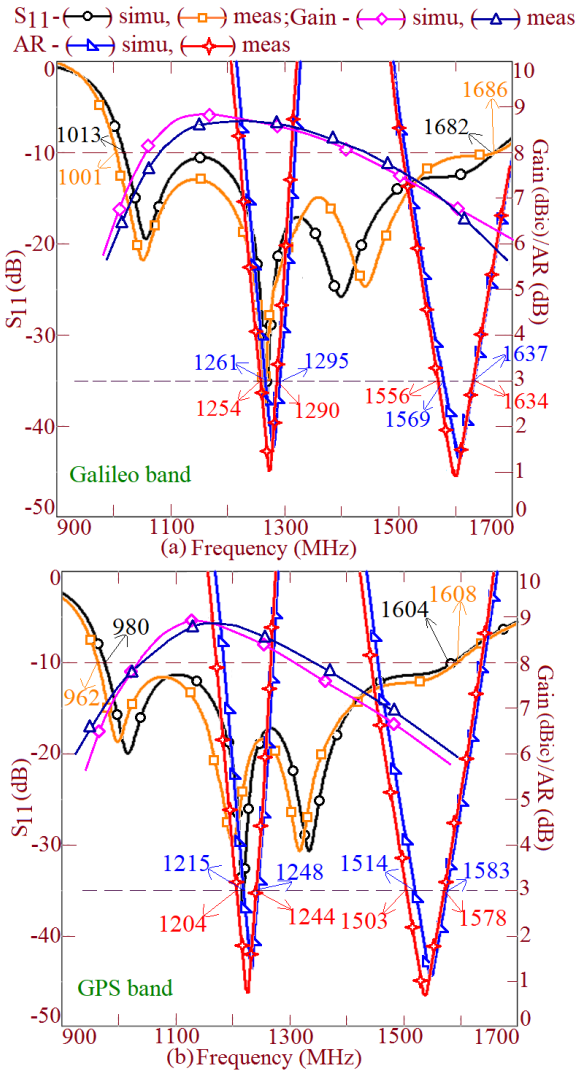

Figure 8. S_{11} & AR BW and gain plots for re-design variations of three rectangular slots cut RMSA in (a) Galileo E and (b) GPS L bands.

Single band CP MSAs discussed in [5, 6] offer lower AR BW, as they were designed on thinner substrate. The circular MSA using E-shape slot offer smaller gain and AR BW [7], whereas dual beam antenna discussed in [8], although employs two patches, but offers AR BW lower than 1%. The shorting pins loaded MSAs for CP response, offer comparatively higher values of the AR BW and gain [9, 10]. However, as per the literature, the gain and BW in MSA reduces when the shorting pins are used [1 – 4]. Therefore, in these designs, which of the shorted patch resonant modes, which gives reported high gain CP characteristics is not clearly mentioned. MSA discussed in [11] give substantially higher value of S_{11} and AR BW. However, reported configuration employs the combination of shorting post, differential feeding with power divider circuit and the proximity feed that together makes the overall design complex. The modified patch shape MSA reported in [12] requires larger patch size and offers smaller BW.

Table 1. Comparison of three rectangular slots cut dual band CP RMSA against the reported MSAs

MSA shown in	Meas. BW (MHz, %)	Meas. AR BW (MHz, %)	A_p/λ_c	Peak Gain (dBi)	h_l/λ_c
Fig. 1(a, b)	685, 51.87	band 1 – 28,2.24 band 2 – 69, 4.39	5.1	band 1 – 8.1 band 2 – 7.2	0.084
Ref [7]	75, 3.15	band 1 – 40, 1.673	4.8	5	0.02
Ref [9]	67, 2.72	band 1 – 16, 0.653	3.5	7.6	0.04
Ref [10]	110, 4.3	band 1 – 34, 1.33	1.91	10.3	0.04

MSA shown in	Meas. BW (MHz, %)	Meas. AR BW (MHz, %)	A_p/λ_c	Peak Gain (dBi)	h_t/λ_c
Ref [11]	2240, 109	band 1 – 1890, 95.2	3.98	6.6	0.07
Ref [12]	35, 2.2	band 1 – 8, 0.5	5.64	3.9	0.02
Ref [13]	653, 54	band 1 – 79, 6.4	> 2.3	8.5	0.11
Ref [14]	450, 27	band – 260, 16	5.3	8.0	0.16
Ref [15]	180, 6	band 1 – 100, 3.3	3.92	2.7	0.03
Ref [16]	360, 9	band 1 – 350, 8.8	3.42	5.8	0.04
Ref [17]	198, 7.95	band 1 – 8, 0.33 band 2 – 18, 0.72	2.23	band 1 – 5.52 band 2 – 6.03	0.04
Ref [18]	255, 15.2	band 1 – 50, 3.2	1.05	4.5	0.15
Ref [20]	175, 7	band 1 – 220, 8.8	3.86	8.7	0.09
Ref [21]	810, 35	band 1 – 130, 5.3	2.36	9	0.1
Ref [22]	2000, 40	band 1 – 1000, 19	3.54	7.5	0.12
Ref [23]	30, 1.9	band 1 – 6, 0.4	1.36	2.3	0.05
Ref [24]	band 1 – 20, 0.9 band 2 – 70, 3.1	band 1 – 12, 0.005 band 2 – 8, 0.004	2.52	band 1 – 7.5 band 2 – 7.5	0.03
Ref [25]	band 1 – 121, 4.99 band 2 – 71, 2.1 band 3 – 402, 9.5	band 1 – 13, 0.53 band 2 – 22, 0.66 band 3 – 36, 0.83	1.24	band 1 – 7.5 band 2 – 8.7 band 3 – 8.7	0.05
Ref [29]	---	band 1: 148, 5.92 band 2: 160, 2.46	---	band 1: 3.8 band 2: 5.5	0.01
Ref [30]	band 1: 130, 5.3 band 2: 470, 13.6	band 1: 70, 2.84 band 2: 55, 1.57	4	band 1: -0.1 band 2: 4.2	0.07
Ref [31]	band 1: 29, 2.99 band 2: 24, 2.72	band 1: 9, 1.07 band 2: 11, 1.19	3	band 1 & 2 > 4.5	0.11
Ref [32]	band 1: 38, 1.8 band 2: 94, 2.6	band 1: 9, 0.4 band 2: 21, 0.6	1.25	band 1: 8.4 band 2: 9.9	0.04
Ref [33]	2000, 37.66	band 1: 550, 11.74 band 2: 374, 6.16	2.25	band 1: 7.0 band 2: 8.3	0.12
Ref [37]	band 1: 100, 4.1 band 2: 245, 7.0	band 1: --- band 2: 62, 1.86	2.268	band 1: 1.38 band 2: 7.1	0.017
Ref [38]	band 1: 162, 5.71	band 1: 60, 2.14	1.44	band 1: 5.5	0.02
Ref [40]	band 1: 350, 14.2 band 2: 800, 13.8	band 1: 500, 20.4 band 2: 550, 9.4	8.997	band 1: 6.4 band 2: 7.5	0.06
Ref [41]	band 1: 13, 1.1 band 2: 27, 2.2 band 3: 40, 2.5 band 4: 62, 2.7	band 1: ---, 4.1 band 2: ---, 1.0 band 3: ---, 1.1 band 4: ---, 1.5	2.864	band 1: 2.23 band 2: 2.91 band 3: 3.40 band 4: 2.70	0.042
Ref [42]	band 1: 210, 4.26 band 2: 290, 5.15	band 1: 50, 1.02 band 2: 70, 1.26	9.11	band 1: 9.0 band 2: 8.6	0.047
Ref [43]	5000, 76.92	band 1: 1200, 23.5 band 2: 1900, 24.2	27.9	band 1: 12.0 band 2: 13.6	0.04

The MSA presented in [13] offers higher values of the BW and gain, but uses offset patches that increase the patch size. The designs reported in [14, 15] employs parasitic patches. Here, the gap-coupled antenna in [14] offers higher CP BW but requires thicker substrate and power divider circuit to create orthogonal input signal conditions. Whereas, in-spite of using parasitic patches, CP antenna in [15] offers lower AR BW. The CP design presented in [16] uses filtering structure to create the additional resonances. The thinner substrate design reported in [17] requires additional coupled lines and offers AR BW less than 1% in the two bands. The CP design employing resonant slot [18 – 21], offer single band CP response and hence cannot find applications in frequency agile applications. The modified slot cut design reported in [22] offers wideband CP response, but does not offer the same in the broadside directions. This causes alignment problem of the antenna against the incoming waves. The fractal shape U-slot cut ground plane design reported in [23] gives AR BW less than 1%. The stub and slot loaded multi-band CP MSAs presented in [24, 25] offer lower AR BW in each band, whereas gap-coupled design discussed in [26] requires large total antenna size. Using printed planar monopole structures, multi-band CP designs are reported [27, 28]. In these configurations, discussion for the functioning of antenna for the modifications employed in the patch geometry with their effects on the resonant modes present, is not put forward. Dual band CP MSA using either shorting post and

slot [30], or the stacked design using multiple patches [31], or gap-coupled design with proximity fed patches [32], offers smaller AR BW in dual bands, as against proposed configuration. The Ψ-shape MSA offering dual band response do not offer CP response in the broadside direction [33]. The use of meta-material units in the CP design loses upon the simplicity of the configuration [34]. The dual band corner truncated slot cut design discussed in [37] offers single band CP response thus does not offer frequency agility needed in wireless communication. The modified ground plane design presented in [38], yields single band CP characteristics. Also, it employs efficient microwave substrate against cheaper substrate selected in the present design. A five-band fractal slot cut corner truncated design is presented in [39]. It offers CP response only in a single band. A dual wideband CP design employing stacked ring patches is discussed in [40]. The multi-layer design employs power divider circuit that increases design complexity and antenna size. Design of four-layer stacked patches offers four band frequency response [41]. Against this, proposed configuration employing single layer single patch, offers dual band CP response. The dual band design discussed in [42, 43] requires larger patch size since it employs longer length of microstrip feed line for patch excitation. In addition to these comparative parameters, in most of the reported work, methodology to design similar configuration for a specific frequency range, is missing. This feature is important as it helps in designing the antenna as per the specific application.

In comparison, proposed design is simple to fabricate, offers dual band response giving small frequency ratio (~1.25). While comparing all the antenna parameters together, i.e. AR BW, gain, antenna volume, and method of realizing CP response, proposed design offers an optimum solution and is useful in applications where the frequency agility is needed. This frequency agility is not possible in reported single slot cut CP MSAs. As compared with the previously reported modified slot cut CP RMSA, proposed MSA offers CP response in the broadside direction, thus removing the alignment problems of the antenna against the incoming waves. A smaller frequency ratio achieved in the proposed CP design, helps in targeting the applications in GPS and Galileo frequency bands as explained above. Thus a simpler unequal lengths rectangular slots cut RMSA design, offering dual frequency circular polarized response in the broadside direction with AR BW of 2 – 5%, is the new contribution in the present study.

As the radiation pattern and broadside gain measurements were carried out inside the antenna laboratory, some degree of variations in the measured antenna parameters exist. The exact duplication of the radiation plots observed in the simulation, is not achieved in the measurements. A variation is noted in the shape of the back-lobe radiation, but the nature of pattern plots remains the same in two cases. But considering all these, a good agreement for the measured results against the simulation is obtained.

5. Conclusions

Multiple rectangular slots cut design of RMSA to offer dual frequency dual sense circular polarized response is presented. The unequal lengths slots in RMSA tune the inter-spacing amongst TM_{10}, TM_{11} and TM_{12} resonant modes, which provide dual frequency and dual sense CP characteristics. Proposed MSA yield S_{11} BW of 50%, with 2 – 5% of the AR BW in dual CP bands, bearing 1.25 of frequency ratio amongst them. Dual band RMSA offer broadside gain greater than 6 dBic over the AR and S_{11} BW with a maximum gain of more than 8 dBic. A design methodology is put forward that helps in realizing similar configurations as per specific frequency applications, like GPS L bands and Galileo E bands. Further, dual band RMSA will be useful in applications, where the frequency agility is required.

REFERENCES

[1] C. A. Balanis, *Antenna Theory: analysis and design*, 2nd edn, USA: John Wiley & Sons Ltd., 1996.
[2] R. Garg, P. Bhartia, I. Bahl, *Microstrip Antenna Design Handbook*, London: Artech House, 2001.
[3] G. Kumar, K. P. Ray, *Broadband Microstrip Antennas*, 1st ed. London: Artech House, 2003.
[4] K. L. Wong, *Compact and Broadband Microstrip Antennas*, 1st ed. New York: John Wiley and Sons, 2002.
[5] Jui-Han Lu and Kin-Lu Wong, "Single-Feed Circularly Polarized Equilateral-Triangular Microstrip Antenna with a Tuning Stub," *IEEE Transaction on Antennas & Propagation*, vol. 48, no. 12, pp. 1869 – 1872, 2000.
[6] P. Nageswara Rao and N. V. S. N. Sarma, "Koch Fractal Boundary Single feed Circularly Polarized Microstrip Antenna," *Journal of Microwaves, Optoelectronics & Electromagnetic Applications*, vol. 6, no. 2, pp. 406 – 413, 2007.
[7] Loo B. K. Bernard, Nasimuddin, and A. Alphones, "An E-shaped slotted-Circular patch antenna for circularly polarized radiation and radiofrequency energy harvesting," *Microwave & Optical Technology Letters*, vol. 58, no. 5, pp. 868 – 875, 2016.
[8] Jiang-Feng Lin and Lei Zhu, "Low-Profile High-Directivity Dual-Beam Circularly Polarized Antennas Under Operation of Two Odd Modes," *IEEE Transaction on Antennas & Propagation*, vol. 70, no. 1, pp. 6 – 16, 2022.
[9] Xiao Zhang, Lei Zhu, and Neng-Wu Liu, "Pin-loaded Circularly-Polarized patch antennas with wide 3-dB axial ratio bandwidth," *IEEE Transaction on Antennas & Propagation*, vol. 65, no. 2, pp. 521 – 528, 2017.
[10] Xiao Zhang and Lei Zhu, "High-Gain circularly polarized microstrip patch antenna with loading of shorting pins," *IEEE Transaction on Antennas & Propagation*, vol. 64, no. 6, pp. 2172 – 2178, 2016.

[11] Chang-Feng Liang, Yun-Peng Lyu, Dong Chen, Wanping Zhang, Chong-Hu Cheng, "A Low-Profile and Wideband Circularly Polarized Patch Antenna Based on TM_{11} and TM_{21}," *IEEE Transaction on Antennas & Propagation*, vol. 69, no. 8, pp. 4439 – 4446, 2021.
[12] Yuzhong Shi and Juhua Liu, "A Circularly Polarized Octagon-Star-Shaped Microstrip Patch Antenna with Conical Radiation Pattern," *IEEE Transaction on Antennas & Propagation*, vol. 66, no. 4, pp. 2073 – 2078, 2018.
[13] Amit A. Deshmukh and K. P. Ray, "Circularly Polarized Designs of Modified Isosceles Triangular Microstrip Antennas," *Engineering Reports*, vol. 2, no. 10, pp. 1 – 16, 2020.
[14] Shiqiang Fu, Qinggong Kong, Shaojun Fang, and Zhongbao Wang, "Broadband Circularly Polarized Microstrip Antenna with Coplanar Parasitic Ring Slot Patch for L-Band Satellite System Application," *IEEE Antennas & Wireless Propagation Letters*, vol. 13, pp. 943 – 946, 2014.
[15] Lin Jiang-Feng and Chu Qing-Xin, "Enhancing Bandwidth of CP Microstrip Antenna by Using Parasitic Patches in Annular Sector Shapes to Control Electric Field Components," *IEEE Antennas & Wireless Propagation Letters*, vol. 17, no. 5, pp. 924 – 927, 2018.
[16] Qiong-Sen Wu, Xiao Zhang, and Lei Zhu, "Co-Design of a Wideband Circularly Polarized Filtering Patch Antenna with Three Minima in Axial Ratio Response," *IEEE Transaction on Antennas & Propagation*, vol. 66, no. 10, pp. 5022 – 5030, 2018.
[17] Zhipeng Zhao, Feng Liu, Jian Ren, Ying Liu, and Yingzeng Yin, "Dual-Sense Circularly Polarized Antenna With a Dual-Coupled Line," *IEEE Antennas & Wireless Propagation Letters*, vol. 19, no. 8, pp. 1415 – 1419, 2020.
[18] Ka Yan Lam, Kwai-Man Luk, Kai Fong Lee, HangWong, and Kung Bo. Ng, "Small Circularly Polarized U-Slot Wideband Patch Antenna," *IEEE Antennas & Wireless Propagation Letter*s, vol. 10, pp. 87 – 90, 2011.
[19] Ahmed Khidre, Kai Fang Lee, Fan Yang, and Atef Z. Elsherbeni, "Wideband Circularly Polarized E-Shaped Patch Antenna for Wireless Applications," *IEEE Antennas & Propagation Magazine*, vol. 52, no. 5, pp. 219 – 229, 2010.
[20] Ahmed Khidre, Kai-Fong Lee, Fan Yang, and Atef Z. Elsherbeni, "Circular Polarization Reconfigurable Wideband E-Shaped Patch Antenna for Wireless Applications," *IEEE Transaction on Antennas & Propagation*, vol. 61, no. 2, pp. 960 – 964, 2013.
[21] Joshua M. Kovitz, HarishRajagopalan, and Yahya. Rahmat-Samii, "Circularly polarised half E-shaped patch antenna: a compact and fabrication-friendly design," *IET Microwave Antennas & Propagation*, vol. 10, no. 9, pp. 932 – 938, 2016.
[22] Tapas Mondal, Sandip Maity, Rowdra Ghatak, and Sekhar Ranjan Bhadra Chaudhuri, "Design and analysis of a wideband circularly polarized perturbed psi-shaped antenna," *IET Microwaves, Antennas & Propagation*, vol. 12, no. 9, pp. 1582 – 1586, 2018.
[23] K. Wei, J. Y. Li, L. Wang, R. Xu, and Z. J. Xing, "A New Technique to Design Circularly Polarized Microstrip Antenna by Fractal Defected Ground Structure," *IEEE Transaction on Antennas & Propagation*, vol. 65, no. 7, pp. 3721 – 3725, 2017.
[24] Neng-Wu Liu, Lei Zhu, Zhong-Xun Liu, Zhi-Ya Zhang, and Guang Fu, "Frequency-Ratio Reduction of a Low-Profile Dual-Band Dual-Circularly Polarized Patch Antenna Under Triple Resonance," *IEEE Antennas & Wireless Propagation Letters*, vol. 19, no. 10, pp. 1689 – 1693, 2020.
[25] Tan Qian and Fu-Chang Chen, "Triband Circularly Polarized Antenna Using a Single Patch," *IEEE Antennas & Wireless Propagation Letters*, vol. 19, no. 12, pp. 2013 – 2017, 2020.
[26] Amit A. Deshmukh, Akshay V. Doshi, and Anuja Odhekar, "Gap Coupled Design Star Shape Microstrip Antenna for Dual Band and Wide Band Circular Polarized Response," *International Journal of RF & Microwave, Computer Aided Engineering*, vol. 29, no. 5, pp. 664 – 674, 2019.
[27] Pawan Kumar, Santanu Dwari, Rohit Kumar Saini, and Mrinal Kanti Mandal, "Dual Band Dual Sense Polarization Reconfigurable Circularly Polarized Antenna," *IEEE Antennas & Wireless Propagation Letters*, vol. 18, no. 1, pp. 64 – 68, 2019.
[28] Fatima Izzat, Aqsa Ahmad, Saqib Ali, Mudassir Ali, and Muhammad Iram Baig, "Triple-Band Circular Polarized Antenna for WLAN/Wi-Fi/Bluetooth/WiMAX Applications," *Progress in Electromagnetics Research C*, vol. 109, pp. 65 – 75, 2021.
[29] Yu Shao and Zhangyou Chen, "A Design of Dual-Frequency Dual-Sense Circularly-Polarized Slot Antenna," *IEEE Transaction on Antennas & Propagation*, vol. 60, no. 11, pp. 4992 – 4997, 2012.
[30] Hong-Yin Zhang, Fu-Shun Zhang, Can Wang, and Tian Li, "Dual-Band Omnidirectional Circularly Polarized Patch Antenna with Etched Slots and Shorting Vias," *Progress in Electromagnetic Research C*, vol. 73, pp. 167 – 176, 2017.
[31] Zhongbao Wang, Ruru She, Junjie Han, Shaojun Fang, and Yuanan Liu, "Dual-Band Dual-Sense Circularly Polarized Stacked Patch Antenna With a Small Frequency Ratio for UHF RFID Reader Applications," *IEEE Access*, vol. 5, pp. 15260 – 15270, 2017.
[32] Zhuo-Xian Liang, De-Cao Yang, Xing-Chang Wei, and Er-Ping Li, "Dual-Band Dual Circularly Polarized Microstrip Antenna With Two Eccentric Rings and an Arc-Shaped Conducting Strip," *IEEE Antennas & Wireless Propagation Letters*, vol. 15, pp. 834 – 837, 2016.
[33] Amit A. Deshmukh and Anuja A. Odhekar, "Dual band Circularly polarized Modified ψ-shape Microstrip Antenna," *Progress in Electromagnetics Research C*, vol. 115, pp. 161 – 174, 2021.
[34] Mohammad Ameen and Raghvendra Kumar Chaudhary, "A compact circularly polarized antenna using CRLH inspired transmission line and coupled ring resonator," *AEU International Journal of Electronics & Communication*, vol. 121, 153238, 2020.
[35] CST Microwave Studio, Version 2019.

[36] Amit A. Deshmukh and A. Odhekar, "Modified Phi-shape Microstrip Antenna For Circularly Polarized Response," *Proceedings of PuneCon 2020*, 16th – 18th December 2020, VIT Pune, India, 2020.
[37] Yang Hongcai and Xiongying Liu, "Wearable Dual-Band and Dual-Polarized Textile Antenna for On and Off Body Communications," *IEEE Antennas and Wireless Propagation Letters*, vol. 19, no. 12, pp. 2324 – 2328, 2020.
[38] Aarti G. Ambekar and Amit A. Deshmukh, "Low Profile Design of Regular Shape Microstrip Antennas Backed by Fractal Slots Cut Ground Plane for Circular Polarized Response," *Progress In Electromagnetics Research C*, vol. 129, pp. 203 – 219, 2023.
[39] Vijayankutty Remya, Manju Abraham, Ambalath Parvathy, and Thomaskutty Mathew, "Multiband Circularly Polarised Microstrip Patch Antenna with Minkowski Fractal Slot for Wireless Communications," *Progress in Electromagnetics Research C*, vol. 116, pp. 65 – 80, 2021.
[40] W. Wang, C. Chen, S. Wang, and W. Wu, "Switchable Dual-Band Dual-Sense Circularly Polarized Patch Antenna Implemented by Dual-Band Phase Shifter of ±90°," *IEEE Transactions on Antennas and Propagation*, vol. 69, no. 10, pp. 6912 – 6917, 2021.
[41] O. P. Falade, M. U. Rehman, X. Yang, G. A. Safdar, C. G. Parini, "Design of a compact multiband circularly polarized antenna for global navigation satellite systems and 5G/B5G applications," *International Journal of RF and Microwave Computer-Aided Engineering*, vol. 30, no. 6, pp. 1 – 13, 2020.
[42] Van Pham Linh, Ta Xuat Son, Nguyen Khac Kiem, Dao-Ngoc Chien, and Nguyen-Trong, Nghia, "Single-Layer, Dual-Band, Circularly Polarized, Proximity-Fed Meshed Patch Antenna," *IEEE Access*, vol. 10, pp. 94560 – 94567, 2022.
[43] Cong Danh Bui, Nghia Nguyen-Trong, and Khang Nguyen Truong, "A Planar Dual-Band and Dual-Sense Circularly Polarized Microstrip Patch Leaky-Wave Antenna," *IEEE Antennas and Wireless Propagation Letters*, vol. 19, no. 12, pp. 2162 – 2166, 2020.

BIOGRAPHY OF AUTHORS

Amit A Deshmukh obtained a BE (Electronics) from VIT, Pune University. He obtained an MTech and PhD from the Department of Electrical Engineering, IIT Bombay. Currently, he is working as Professor & Head of the Department of Electronics and Telecommunication Engineering at D. J. Sanghvi College of Engineering, Vile-Parle (W), Mumbai, India. He has published more than 250 journal and conference papers.

Tejal P. Page has done her post graduation in electronics and telecommunication engineering from Mumbai University. Her field of specialization is microstrip antennas. She has around 6 journal papers and 13 conference papers to her name. She has been working as an assistant professor with Mumbai University college for past 12 years.

Venkata A P Chavali received BE degree in Electronics and Communication Engineering from Andhra University, Vishakhapatnam, India in 2004 and ME degree in Digital Communication from RGPV, Bhopal, India in 2010, and PhD degree in Electronics and Telecommunication Engineering from D J Sanghvi College of Engineering, Mumbai University, in 2022. Since 2012 she has been working as Assistant professor with the Electronics and Telecommunication Engineering Department, D J Sanghvi College of Engineering, Mumbai, India. Her research interest includes broadband microstrip antennas. She has 30 Journal and about 50 conference publications to her credit.